Composites Part C: Open Access 10 (2023) 100339

Contents lists available at ScienceDirect

Composites Part C: Open Access

journal homepage: www.sciencedirect.com/journal/composites-part-c-open-access

Multi-functional Composites

Investigation of mechanical recycling effect on electromagnetic properties of polylactic acid (PLA) – nanoclay nanocomposites: Towards a valorization of recycled PLA nanocomposites

Lakhdar Sidi Salah [a,*], Nassira Ouslimani [b], Yann Danlée [c], Freddys R. Beltrán [d], Isabelle Huynen [c], María Ulagares de la Orden [e]

[a] Research Unit Materials, Processes and Environment (URMPE), Faculty of Technology, M'Hamed Bougara University, 35000 Boumerdes, Algeria
[b] Processing and Shaping of Fibrous Polymers Laboratory, Faculty of Technology, University M'Hamed Bougara of Boumerdes, Avenue of Independence, Boumerdes 35000, Algeria
[c] Institute of Information and Communication Technologies, Electronics and Applied Mathematics (ICTEAM), Université catholique de Louvain, 1348 Louvain-la-Neuve, Belgium
[d] Escuela Técnica Superior de Ingenieros Industriales, Universidad Politécnica de Madrid, 28006 Madrid, Spain
[e] Facultad de Óptica y Optometría, Universidad Complutense de Madrid, 28037 Madrid, Spain

ARTICLE INFO

Keywords:
Polymer-matrix composites
Recycling
Electric properties
EMI Shielding
Particle-reinforcements

ABSTRACT

Virgin and recycled poly(lactic acid) (PLA) based nanocomposite materials were obtained and subjected to microstructural, thermal and mechanical analysis in view of fabricating efficient microwave absorbers. PLA was first exposed to artificial accelerated aging, next was mechanically recycled through grinding followed by reprocessing using melt extrusion and compression molding, resulting in recycled PLA samples (rPLA). Addition of organically modified montmorillonite (OMMT) as nanoclay was performed in a second melt extrusion process in order to obtain virgin and recycled PLA-OMMT nanocomposites. The impact of recycling process and presence of OMMT nanoclay in the host PLA matrix has been studied by FTIR, TGA and DSC, while the mechanical performance has been investigated by micro-hardness test. The dielectric properties were measured in the 26–40 GHz frequency range using a Vector Network Analyzer to assess the performance of virgin and recycled PLA and OMMT-PLA material as microwave absorbers. The FTIR results show that the recycling process generated more C = O groups in the polymer. These polar groups tend to orient themselves in the direction of the applied field and increase the dielectric constant (ε'). Measured electromagnetic absorption index revealed that rPLA-4OMMT with a thickness of 400 μm is able to absorb 20.3% on average of the spectrum with a peak of 36%, while 200 μm-thick films of rPLA-4 wt.% OMMT has a mean absorption index of 14.5%. The overall results show that mechanically recycled polymer can replace virgin polymer in this kind of applications.

1. Introduction

The primary purpose of the European Parliament in 2019 for promoting a circular economy of materials includes the use of biodegradable materials, aiming to reduce the world's plastic growing waste [1]. For applications such as fibers, textiles, food packaging, and environmental remediation films, poly(lactic) acid (PLA) is the most promising alternative for reducing municipal solid waste [2]. PLA, on the other hand, has some drawbacks, such as poor toughness, brittleness and high gas permeability, so intensive research efforts are focused on obtaining PLA products with specific properties. This can be achieved by blending PLA with other biodegradable and non-biodegradable resins, and/or by compounding PLA with fillers such as montmorillonite (MMT) nanoclay [3] [4]. MMT is a widely used layered silicate (MLS), usually modified with different alkyl ammonium ions to produce organically modified MMT (OMMT), which is frequently incorporated in PLA-based materials forming PLA-OMMT hybrid nanocomposites with improved characteristics [5] [6].

MMT consists of sheets arranged in layered structure with high aspect ratio particles with at least one dimension in the nanometer range, which significantly improves the properties of the PLA polymer. The organically modified layered silicates (OMLS) are employed as

* Corresponding author.
E-mail address: l.sidisalah@univ-boumerdes.dz (L.S. Salah).

https://doi.org/10.1016/j.jcomc.2022.100339

Available online 13 December 2022

reinforcements because of their high cation exchange capacity (CEC) and high surface area (approximately 750 m^2/g) with a platelet thickness of 10 Å. The large aspect ratio of the silicate layers results in a high interfacial area. This increase in the interface reduces the chain mobility and creates a reinforcement effect [7] [8] [9]. The affinity of silicates with PLA is reported to be strong [10], presuming of a good compatibility between them. Nanocomposites present improved mechanical and gas barrier properties when the optimum amount of filler is reached, which is usually in the 1 – 5 wt.% range [11]. This is an advantage since mechanical properties are reported to degrade at too high filler content. The positive effects of OMLS promoted the use of silicate-based nanocomposites in both academic and industrial field, as they exhibit a remarkable improvement in the properties of materials compared to pure PLA or conventional composites [12] [13]. Those improvements may include higher moduli [14], increased resistance to heat, decreased gas permeability and flammability, and increased biodegradability [15] [16]; the improvement of these properties is dependent on a few parameters, including clay distribution (such as dimensions, form factor, exfoliation, etc.), which favor higher reinforcement via nanoclay-polymer interaction.

This growing trend in the consumption of PLA-based materials could create some environmental issues. Most commercial grades used in demanding applications, such as food packaging, do not easily biodegrade in ordinary conditions [17] and can also be considered as a contaminant for polyethylene terephthalate (PET) waste streams [18]. To address this issue, several alternatives for the valorization of plastic waste have been proposed and evaluated, such as mechanical recycling [19]. Mechanical recycling is one of the most successful processes, and it has received a lot of attention because of its key advantages, such as its simplicity, inexpensive investment, and controllable technological parameters [20]. Nevertheless, polymers and nanocomposites are known to be degraded by agents such as oxygen, light, mechanical stresses, temperature and water, which in combination cause chemical and physical changes that alter their structure during their life cycle (synthesis - processing - service life - discarding - recovery) [20] [21]. As a result of these changes, the physical and functional properties of a polymer deteriorate. Hence, high quality recycled products are difficult to obtain, in particular for thin films, where optical and barrier qualities, among other issues, play an important role [22] [23]. However, the performance of the mechanically recycled plastics can be still enough to be used in different applications. Moreover, the addition of OMMT in the reprocessing step can result in a substantial improvement of the properties of the recycled PLA.

To the best of our knowledge the use of recycled materials for the fabrication of microwave devices including absorbers is a new research field not yet deeply investigated. In this work, virgin and recycled PLA-based OMMT nanocomposites have been obtained and characterized using different experimental techniques, such as FTIR spectroscopy, thermogravimetric analysis (TGA), differential scanning calorimetry (DSC) and microhardness measurements. The main goals were to investigate the effects of the nanofiller and the recycling process on permittivity and dissipation factors of the materials, since the dielectric properties should be adapted for ensuring microwave absorption and electromagnetic interference (EMI) shielding, and to evaluate the suitability of using formulations based on mechanically recycled PLA, instead of those based on virgin polymers, as biodegradable electronic materials for efficient microwave absorbers operating in K_a band.

2. Materials and methods

2.1. Materials

The PLA used was a commercial grade, Ingeo™ Biopolymer 2003D, from NatureWorks (USA), with a melt mass-flow rate of 6 g/10 min (2.16 kg at 210°C). A commercial organically modified montmorillonite (OMMT), Cloisite® 30B from Southern Clay Products (USA), modified with a methyl, dihydroxyethyl, dehydrogenated tallow, quaternary ammonium chloride, was used as a filler.

2.2. Preparation of the materials

PLA pellets were processed by melt extrusion in a Rondol Microlab twin-screw microcompounder ($L/D = 20$), at 60 rpm. The temperature profile, from hopper to die was: 125–165–190–190–180 °C. The obtained material was then hot-pressed into films (thickness of 200 μm) using an IQAP-LAP hot plate press at 190 °C. The obtained films of virgin PLA (VPLA) were then subjected to an accelerated aging protocol including 40 h of photochemical aging in an ATLAS UVCON chamber, equipped with eight F40UVB lamps; 480 h of thermal aging in an oven at 50 °C; and 240 h of hydrolytic aging in deionized water at 30 °C. The aged samples were then washed at 85 °C in a NaOH (1 wt.%) and Triton X (0.3 wt.%) aqueous solution. Finally, the washed material was grinded and reprocessed by melt extrusion and compression molding, resulting in recycled PLA (rPLA). The addition of OMMT was performed in the second melt extrusion process. The Table 1 summarizes the elaboration of the samples and gives a short sample name used further in this paper.

In order to avoid humidity traces, all the materials were dried at 85 °C under vacuum for 2 h before processing.

3. Characterization of the samples

Fourier transform infrared (FTIR) spectra was recorded in a Nicolet iS10 spectrometer, equipped with a diamond ATR accessory. For each sample, 16 scans with a resolution of 4 cm^{-1}, were recorded. FTIR-ATR spectra were corrected using the software Omnic 9.2.41 and normalized using the band at 1450 cm^{-1}, which has been reported as an internal standard.

Differential scanning calorimetry tests (DSC) were conducted in a TA Instruments Q20 calorimeter, under nitrogen atmosphere. 5 mg of sample were put in a standard aluminum pan, and subjected to the following protocol:

- A heating scan, from 30 to 180 °C, at 5 °C/min.
- An isothermal step at 180 °C for 3 min.
- A cooling scan, from 180 to 0 °C, at 5 °C/min.
- A second heating scan, from 0 to 180 °C, at 5 °C/min.

Thermogravimetric analysis (TGA) was carried out in TA Instruments TGA 2050 thermobalance under nitrogen atmosphere. 10 mg of sample were put in a platinum crucible, and heated from room temperature to 800 °C, at 10 °C/min.

Hardness measurements were performed in Shimadzu Type M microhardness tester, equipped with a Vickers pyramidal indenter. The applied load was 25 g and the loading time was 10 s. Each sample was measured six times.

The electromagnetic characterization is performed over the K_a band by using an Anritsu M54644B Vector Network Analyzer (VNA) in wave guide configuration as described in ref. [24]. The calibration is made by

Table 1
Description of the studied samples.

Sample	Description
VPLA	PLA subjected to an extrusion and compression molding process
VPLA-2OMMT	PLA + 2 wt.% OMMT subjected to an extrusion and compression molding process
VPLA-4OMMT	PLA + 4 wt.% OMMT subjected to an extrusion and compression molding process
rPLA	VPLA subjected to accelerated aging, washing and reprocessing
rPLA −2OMMT	VPLA subjected to accelerated aging, washing and reprocessing along with 2 wt.% OMMT
rPLA −4OMMT	VPLA subjected to accelerated aging, washing and reprocessing along with 4 wt.% OMMT

LRL/LRM method, and the IF bandwidth is set at 300 Hz. The VNA measures the parameters S_{11} and S_{21} associated to power respectively reflected ($R=|S_{11}|^2$) at input of the material sample and transmitted ($T=|S_{21}|^2$) through it. These raw S-parameters are converted towards reflection and transmission coefficients for the absorption analysis. From the power balance $A+R+T=1$, the absorbed power A is obtained as $A=1-R-T$. These definitions are used in Section 4.5.2.

4. Results and discussion

4.1. FTIR analysis

FTIR spectroscopy makes it possible to characterize the functional groups in polymers by identifying their absorption bands and, hence, to investigate the interactions between the different substances present in the plastic and the modifications caused by processes such as the degradation that take place during the use and the mechanical recycling of the plastic. FTIR spectroscopy analysis was performed on samples of PLA and PLA-based nanocomposites before and after being subjected to recycling, and the results are displayed in Figs. 1 and 2.

All the spectra are very similar and show the characteristic absorption bands of PLA, previously reported by Kister, G et al. [25]. This result indicates that the recycled polymer is very similar to the virgin one, at least from a chemical structure point of view. However, there are small changes that can be related to the recycling process. For example, the two weak absorption bands observed around 2998 and 2948 cm^{-1}, which correspond to the stretching modes of aliphatic C—H bonds [26], are shifted to lower wavenumbers for rPLA. This change can be related to small changes in the surface crystallization of the material [27,28] . The peak at 1755 cm^{-1} corresponds to the C = O stretching vibration of the ester group [29]. After recycling the pure polymer, a small change can be appreciated in this region (Fig. 2). The spectrum of recycled plastic is slightly broader in this spectral region. The two spectra are equal at high wavenumbers; however, the spectrum of recycled plastic is slightly broader at low wavenumbers, showing the appearance of lower energy C = O bonds because of recycling. This fact could be due to the cleavage of chains in the polymer during its aging and reprocessing, which causes the formation of acid and alcohol groups. These new groups can establish hydrogen bonds with the C = O of the ester groups of PLA, thus lowering the energy of the vibration. Thus, the changes observed in the spectrum of rPLA in comparison to VPLA, can be attributed to degradation processes that generate new C = O groups. These changes are in good agreement with the reduction in molecular weight by chain scission in the recycled polymer, which has been reported by different authors [30,31].

Fig. 2 also shows the C = O spectral region corresponding to virgin and recycled PLA nanocomposites with 4 wt.% of OMMT. In this case, the difference observed between VPLA and rPLA, which can be assigned to degradation by chain scission, do not appear. However, it is well known that chain scission also takes place during the aging and mechanical reprocessing of the nanocomposites, as can be deduced from the measurements of intrinsic viscosities and average molecular weights of these materials [31]. The non-observation of the new hydrogen bonds in the recycled nanocomposites may be due to the nanoclay layers since they make it difficult to establish interactions of this type in the polymer.

4.2. Thermogravimetric analysis

Thermogravimetric analysis (TGA) is a quantitative analysis that relies on the mass change of a material exposed to a controlled temperature program. Analyzing the thermal stability of the different is important, since it has been reported that the introduction of inorganic nanoparticles into polymers leads to improvement on the thermal stability of the samples [32].

The TG traces and respective derivative mass loss (or derivative thermogravimetry, DTG) of all the investigated samples are presented in Fig. 3. The TG curves show that the degradation process occurs in a single weight-loss step for all the samples. The decomposition of PLA starts at around 300 °C. The decomposition is rapid above this temperature, and it completes at 380 °C. The DTG curve of PLA in Fig. 3b shows a single peak at 365 °C.

Table 2 summarizes the TGA characteristic temperatures of the different PLA samples. Thermal stability of the prepared formulations is quantitatively characterized from $T_{5\ -\ 50}$ (temperatures of 5 and 50% weight loss) and T_{max} (temperature of maximum weight loss rate), which are commonly used as indicators for the thermal stability of polymers. Table 2 shows that the recycling causes a decrease in the thermal stability of PLA. The result has been reported in previous studies, and it is related to the degradation of PLA during the aging and recycling process. This degradation has been also observed in the FTIR analysis of the materials (Figs. 1 and 2). The samples with lower molecular weight have shorter polymer chains, which decompose at lower temperatures, negatively affecting the thermal stability [33]. The presence of the nanoclay filler leads to slight changes in thermograms; overall the addition of 2 and 4 wt.% of OMMT led to a slight increase of the thermal stability of the virgin and recycled PLA matrixes, as it can be seen on Table 2 and Fig. 3. In fact, the introduction of 2 wt.% OMMT during the recycling PLA process can significantly improve the thermal stability of the recycled nanocomposites approaching the thermal stability of virgin PLA matrix. It is reported elsewhere that thermal stability of PLA can be enhanced or decreased by the introduction of OMMT [34,35]. Regarding the DTG curve and the T_{max} values, one observes that the addition of 2 and 4 wt.% led to a slight increase of the T_{max} values of the recycled matrix. This improvement of the thermal stability might indicate a good dispersion of the clay platelets within the polymer matrix, since they can act as a barrier to the liberation of the thermal

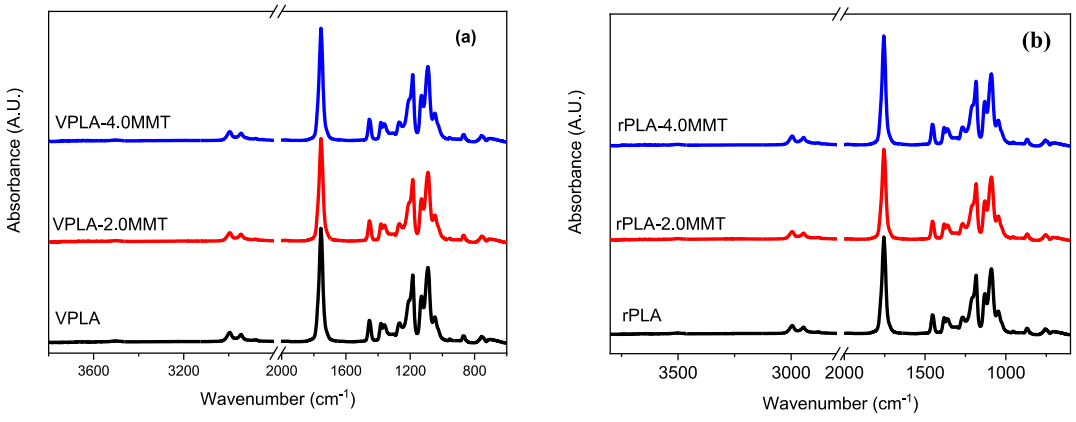

Fig. 1. FTIR analysis of virgin and recycled PLA-nanoclay composites.

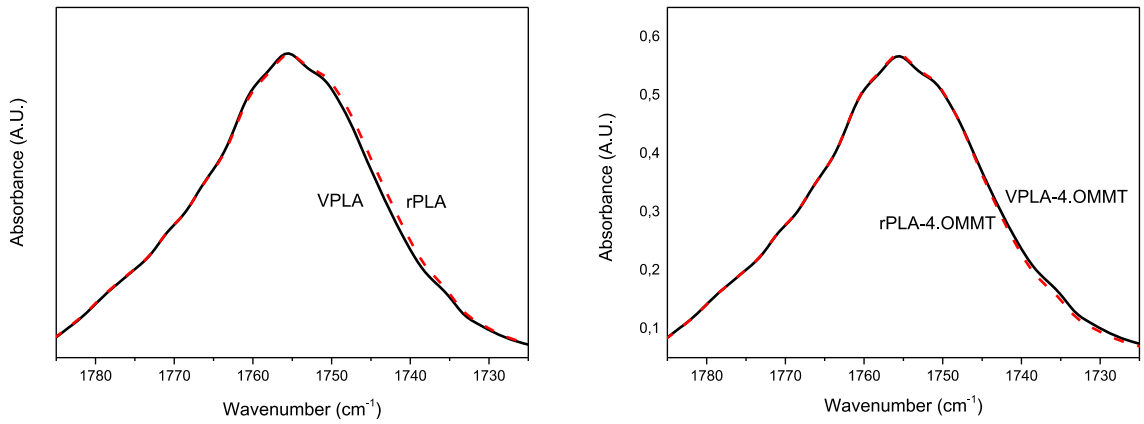

Fig. 2. FTIR analysis over the 1790 – 1720 cm^{-1} wavelength, the full black line and the dotted red line are the virgin and recycled PLA-based composites respectively. The change in the C = O stretching region is caused by the recycling process.

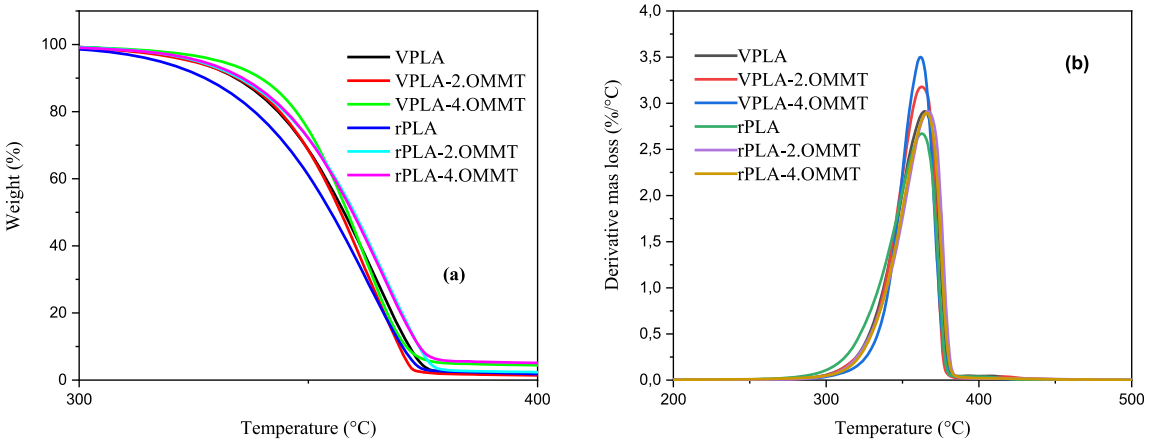

Fig. 3. TGA (a) and DTG (b) analysis for PLA based samples.

Table 2
The TGA characteristic temperatures of the different PLA based samples.

Sample	T_5(°C)	T_{50}(°C)	T_{max}(°C)
PLA	325, 39	357, 81	364, 37
PLA-2OMMT	324, 66	357, 06	362, 38
PLA-4OMMT	330, 88	358, 56	361, 86
rPLA	317, 60	354, 95	362, 6
rPLA-2OMMT	325, 89	360, 0	366, 71
rPLA-4OMMT	326, 69	359, 67	365, 86

decomposition products. The enhancement of the thermal stability thus reveals a good interaction between the inorganic layered silicates and the PLA matrix in the fabricated nanocomposites [36–39] .

Summarizing, mechanical recycling led to a decrease of the thermal stability, as a result of the degradation of the polymer. Nevertheless, the presence of nanoclay is positive as the poor thermal stability of rPLA is synergistically recovered by the introduction of low content of organically modified OMMT that is considered sufficient to induce better thermal stability.

4.3. DSC characterization

DSC analysis was performed in order to evaluate the effect of mechanical recycling on the thermal transitions and crystalline structures of the polymer matrix during the recycling process. Thermograms are shown in Fig. 4 and followed by Table 3 summarizing the characteristic data: melting temperature (T_m), cold crystallization temperature (T_{cc}),

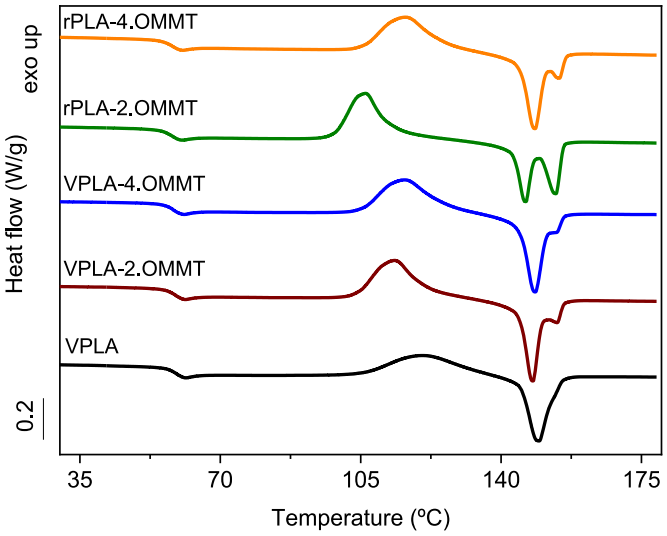

Fig. 4. DSC second heating scans of PLA-based samples.

enthalpy of crystallization and melting, respectively (ΔH_c and ΔH_m) and the degree of crystallinity (X_c) based on the second heating cycle. Fig. 4 shows that, overall all the samples present the same thermal transitions, namely a glass transition around 60 °C, a cold crystallization above 100 °C and a melting endotherm above 140 °C. Despite the similarities,

Table 3
The characteristic data exported from second scan heating of PLA-based materials.

Sample	T_g(°C)	T_{cc}(°C)	T_m(°C)	ΔH_{cc}(J/g)	ΔH_m(J/g)	X_c(%)
VPLA	57, 98	120, 4	149, 49	22, 67	22, 87	0
VPLA-2OMMT	57, 84	113, 46	147, 89 – 153, 97	27, 46	28, 4	1
VPLA-4OMMT	57, 32	115, 96	148, 5	28, 04	28, 54	1
rPLA	57, 27	109, 79	146, 98 – 153, 60	28, 2	29, 5	1
rPLA-2OMMT	56, 70	106, 22	146, 13 – 153, 66	29, 1	29, 4	0
rPLA-4OMMT	56, 96	116, 15	148, 43 – 154, 55	27, 7	28, 0	0

there are some differences that are worthy to note. Recycled PLA shows a cold crystallization temperature approximately 10 °C lower than VPLA. This behavior has been reported in previous studies [27,33], and can be attributed to the degradation of the polymer during the aging and recycling, since the shorter polymer chains have an increased mobility which allows them to crystallize more easily. Another important difference is the double melting peak shown by the recycled materials. This behavior can be assigned to a melt recrystallization mechanism, as it was pointed out by Di Lorenzo [40]. In this mechanism, the crystals formed during the cold crystallization partially melt, reorganize themselves into more perfect crystals and then melt at a higher temperature. The appearance of this behavior in the recycled material can also be attributed to the shorter polymer chains with higher mobility, which can rearrange themselves more easily during the melt recrystallization.

Regarding the effect of the nanoclays, two counteracting effects on the T_{cc} can be seen depending on the amount of filler. In the samples with only 2 wt.%, a decrease of the cold crystallization temperature was noted. This behavior can be ascribed to the clay nanoparticles providing heterogeneous crystallization sites for PLA, thus promoting the formation of crystalline structures at lower temperatures [41–44] . As the clay content increases, so does the T_{cc} value, which could be explained by a decrease of the mobility of the molecular segments due to the presence of the nanoclay platelets. Similar behaviors have been reported for PLA-organically modified clay nanocomposites [45–47].

4.4. Micro-hardness measurements

Microhardness is an important mechanical property that measures the resistance of a material to the application of a contact load; it could also provide valuable information about morphological parameters of polymers [48,49]. As it can be seen in Fig. 5, the value of Vickers hardness of VPLA is around 185 MPa, which is approximately 5 MPa higher than the one of rPLA. This slight decrease is related to the degradation of the polymer during recycling, since molecular weight is one of the factors that influences mechanical performance [50]. Fig. 5 also shows that the addition of both 2 and 4 wt.% OMMT to rPLA led to nanocomposites with hardness values even higher than those of unfilled VPLA. These results might be explained by the presence of high aspect ratio montmorillonite nanoparticles, since the high surface area of nanoparticles promotes increase in hardness of hybrid PLA nanocomposites [51]. Furthermore, as it was seen by means of DSC, the nanoclay tends to restrict the movement of polymer chains, thereby increasing the microhardness [52]. These results are important since they suggest that the addition of small amounts of nanoclay can improve the mechanical performance of mechanically recycled PLA.

4.5. Electrical and electromagnetic behavior

4.5.1. Dielectric properties

The variation with GHz-frequency of the dielectric constant (ε') and the dissipation factor (tan δ) of the polymer nanocomposites was measured at room temperature (22.5 °C) using a vector network analyzer operating in the range of 26.5–40 GHz (K_a band) and presented in Fig. 6. The maximum values of ε′ are found at lower frequencies; the ε' value of VPLA is in the range 2.9–3.9 while rPLA displayed some fluctuations and its value is in the range 2.9–4.4. The average values ε' in the studied frequency band for VPLA and rPLA are 3.1 and 3.8, respectively. Note that the experimental oscillations are due to a slight impedance mismatch over the swept frequency range. Furthermore, the algorithm for extracting the physical properties from S-parameters inevitably amplifies these oscillations [53]. The behavior of ε' is attributed to the dominant contribution of the Maxwell-Wagner-Sillars interfacial polarization (effect Shetty) typically observed in certain polymers [54,55]. Indeed, charges accumulation at interfaces of dielectric samples improve the dielectric polarizability [56], and this behavior seems more

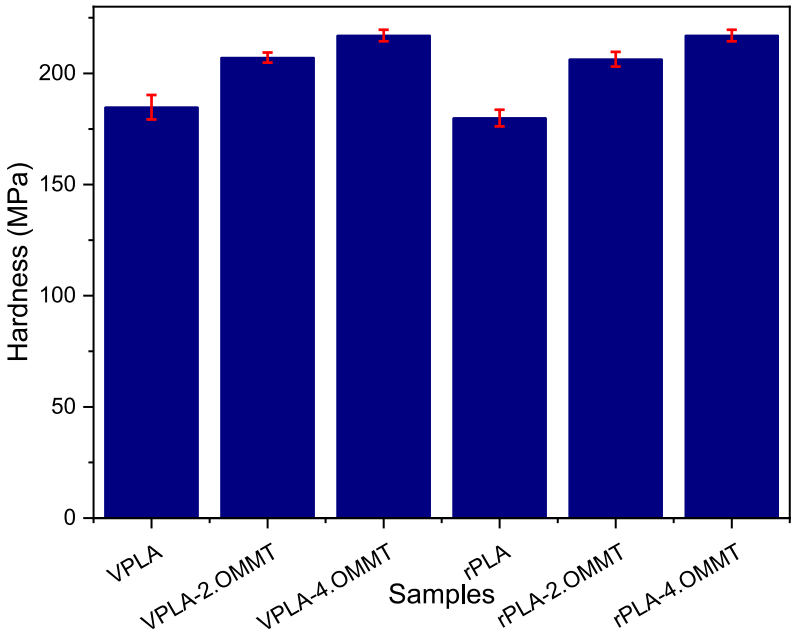

Fig. 5. Microhardness of PLA-based materials.

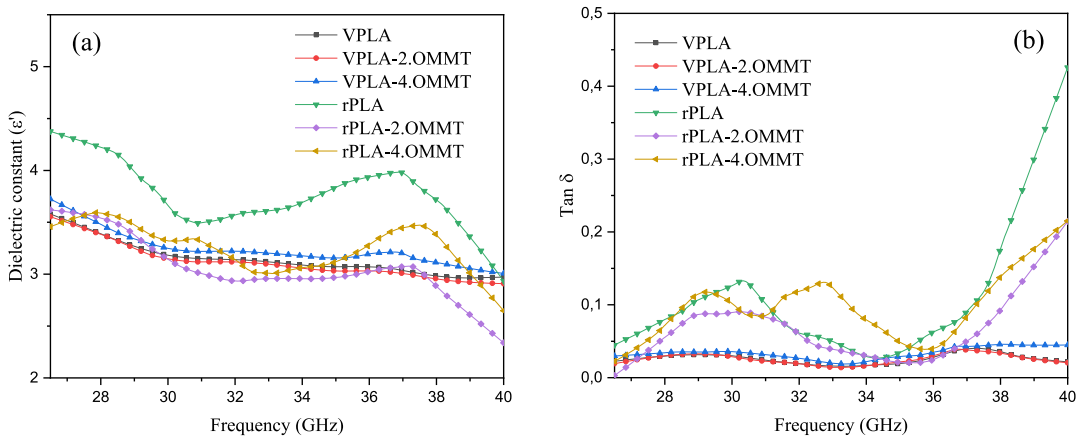

Fig. 6. Dielectric constant (a) and loss tangent (b) at microwave frequencies of PLA-based composites over the K_a band.

pronounced for rPLA formulations. The phenomenon can be viewed as the existence of small electrical capacities between OMMT inclusions loading the material, which contributes to the modification of values ε' [57]. At low frequency, the capacitance increases the effective value of ε', while at high frequency, the capacitance act as a short circuit between inclusions in the PLA matrix, leading to a gradual decrease of ε' when frequency increases; a steady state is reached near 30–33 GHz and 32–35 GHz for PLA samples and rPLA-2OMMT, respectively. Any composite exposed to an alternating electric field is characterized by interfacial and orientation polarization, these two physical characteristics mainly govern the dielectric constant value. On the one hand, it is reported that dipoles get enough time to orient themselves in the direction of applied electric field at lower frequency [58,59]. On the other hand, as the frequency increased, the dipoles get less time to orient them in the direction of the applied electric field reducing by that interfacial and orientation polarization hence lowering the dielectric constant [60]. Mechanical recycling induces the formation of small chains, having more polar groups than in VPLA as confirmed from FTIR analysis, hence the polarization and the capacity of dipoles to orient themselves in the same direction as the electrical field is enhanced. Consequently, the value of ε' of rPLA samples kept increasing again at 32 GHz.

Regarding the behavior of the nanocomposites, it is worth noting that OMMT is polar in nature, thus a decrease of dielectric constant is related to the exfoliation/intercalation of the nanoclay in the PLA host matrix, involving the reduction in dielectric constant and dissipation factor for 3 wt.% nanoclay is due to immobility of PLA chains by nanoparticles [61]. The exfoliated nanoclay decreases the dielectric constant of nanocomposite whereas dielectric constant increases due to predominance of intercalated clay. Consequently, the orientation of polar dipoles present in the rPLA matrix is somewhat suppressed due to the hindrance created by MMT in their movement, this behavior is clearly seen for all PLA materials in the frequency range 26.5–32 GHz. However, nanoclay can increase interfacial polarization, but this phenomenon is dominated by orientation polarization as it is evident for both virgin and recycled nanocomposites at 35 GHz. Thus, ultimately, the suppression of orientation polarization reflects the decrease in dielectric constant and dissipation factor with the increase in nanoclay loading. It has been suggested in previous studies that the presence of polar groups in conductive nanoparticles platelets can increase the dielectric constant by the impartial relatively high permanent dipole moment and high interface polarizability of these bonds, additionally the presence of electronegative atoms in nanoparticles sheets causes a doping effect increasing the conductivity of the composites [62]. A similar trend has been seen in the case of rPLA, which can be explained by the C = O groups, with high dipole moments, created during recycling. These C = O groups contribute to high values of AC conductivity and dielectric constant, as it can be seen from average AC conductivity results that are summarized in Table 4. The addition of clay does not produce important changes in AC conductivity, thus it must be the generation of new compounds with C = O bonds, both in the middle position and at the ends of the PLA chains, the responsible for the rise in dielectric properties of both recycled matrix and nanocomposites. From Table 1, it can be seen that values of conductivity or one order of magnitude higher for recycled PLA composites, with values up to 1 S/m for rPLA-4OMMT. Those results are satisfactory for achieving EMI shielding as high as 30 dB according to [52].

4.5.2. *Electromagnetic (EM) absorption index*

The performance of polymer-nanofiller composites to shield electromagnetic (EM) radiation is evaluated by measuring S-parameters followed by specific data extraction algorithm [53,63]. These parameters have been extracted from a vector network analyzer (VNA) operating in the K_a band (26.5–40 GHz). Recent studies have claimed that the presence of nanosilica particles within a coating will boost its durability, due to the strong potential of nanosilica to absorb ultraviolet (UV) radiation, which prevents the deterioration of the organic polymeric covering [64]. The ability of PLA and recycled PLA based nanocomposites to absorb electromagnetic radiation could prove useful, since absorption is the only way to remove undesired pollution [65]. The shielding effectiveness generally is correlated to the electromagnetic transmission and consequently does not give information about the reflection. A strong reflection resend microwave without solving interference issues since no energy absorption is done. In this aim of EMI shielding, PLA and rPLA nanocomposites with a thickness of 200 and 400 μm were characterized, and the results are displayed in Fig. 7. From S-parameters, the reflection (R) and transmission (T) coefficients are calculated, then the absorption index (A) is obtained by the formula $A = 1 - R - T$ where $R = |S_{11}|^2$ and $T = |S_{12}|^2$.

The reflection coefficient of the set of films is quite weak. This is an advantage since the energy penetrate into the material for partial absorption and transmission. Notice that the thickness increases the reflection; this is explained by the fact that a thicker film offers a higher content in lossy PLA-OMMT material for the propagation of the signal.

Table 4
Average conductivity and dielectric constant at microwave frequency of the nanocomposites.

Sample	Conductivity [S/m]	Dielectric constant
VPLA	0.06	3.0
VPLA-2OMMT	0.12	3.1
VPLA-4OMMT	0.16	3.3
rPLA	0.77	3.4
rPLA-2OMMT	0.83	3.3
rPLA-4OMMT	1.00	3.5

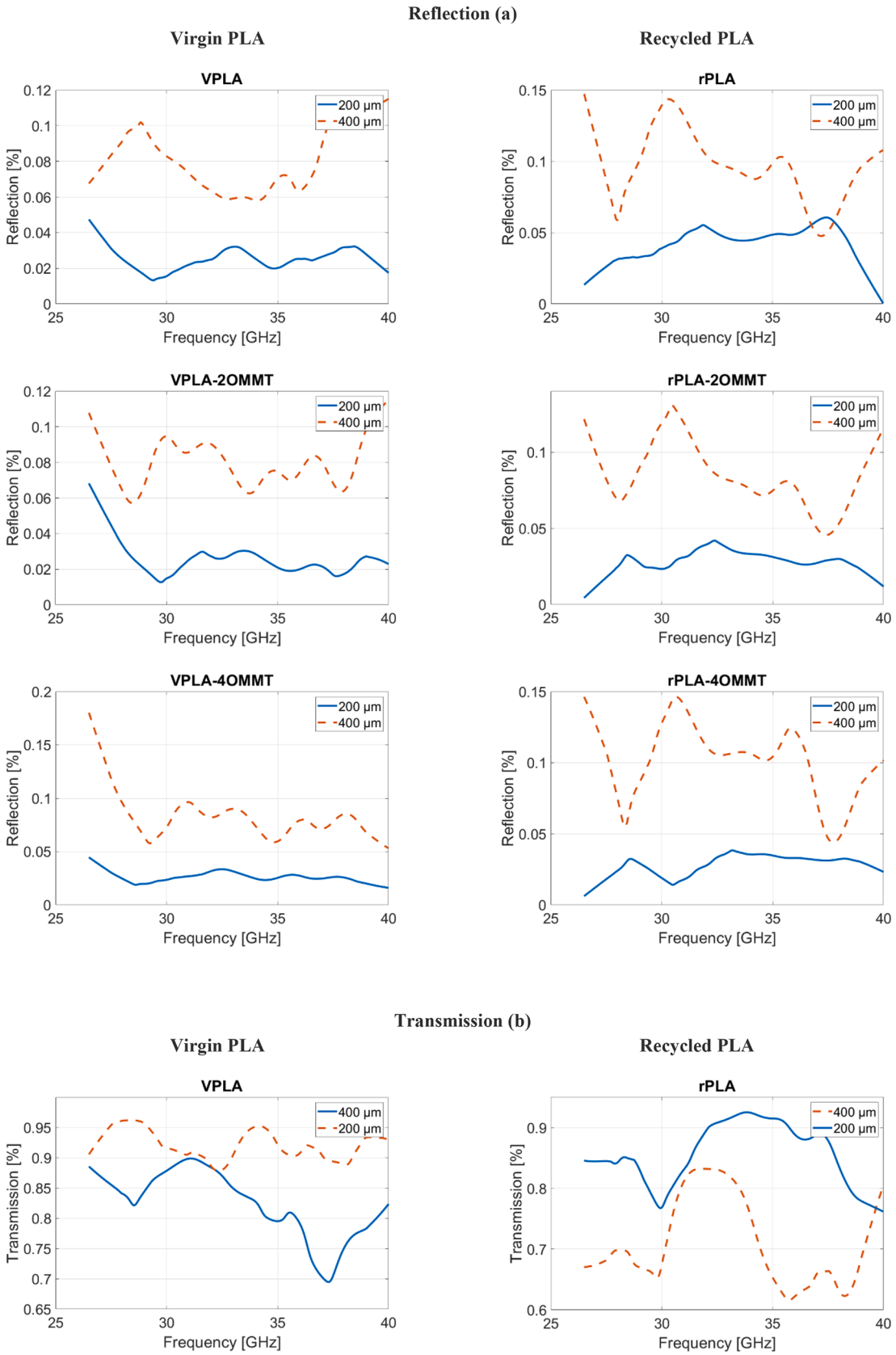

Fig. 7. Electromagnetic reflection (a), transmission (b) and absorption index (c) of PLA-based composites with a thickness of 200 and 400 µm over K_a frequency band.

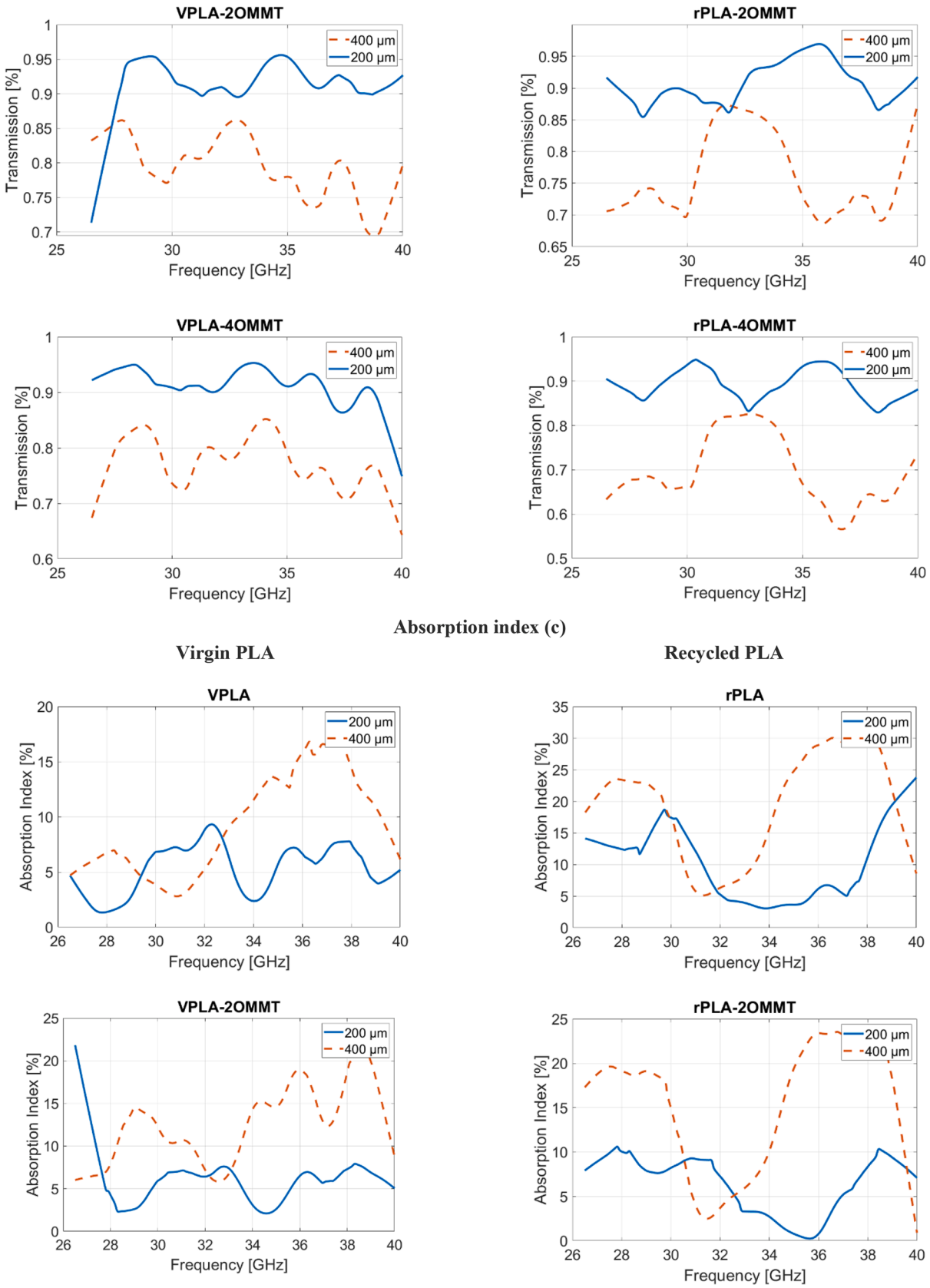

Fig. 7. (*continued*).

The films being seriously smaller than the wavelength are seen by the signal as a thin conductive layer with lower shielding power than metal. The value of transmission for VPLA at 200 µm fluctuates between 0.90 and 0.88 where the lowest and highest values 0.90 and 0.93 are attained at 26.5 and 40.0 GHz. For rPLA, the value of T is between 0.75 and 0.90 between 26.5 and 40 GHz. The addition of 2 wt.% significantly reduced

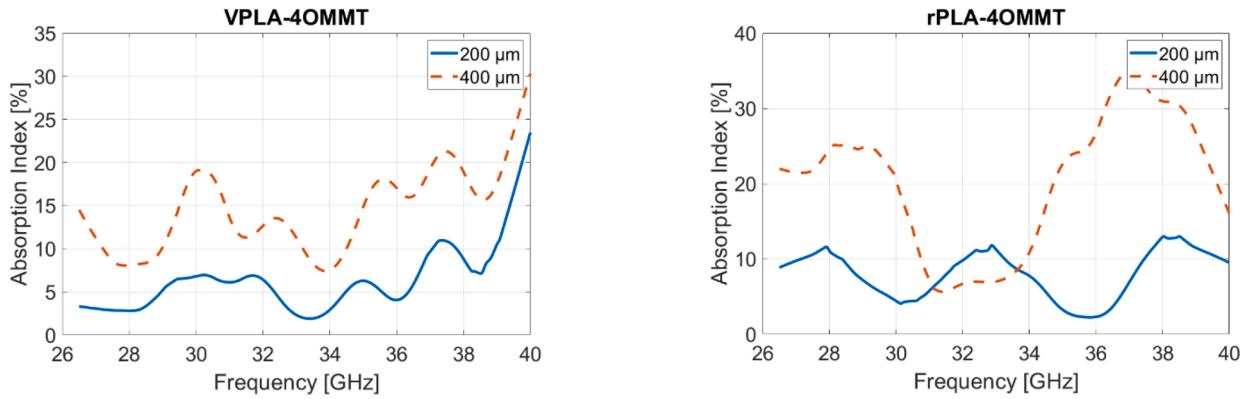

Fig. 7. (*continued*).

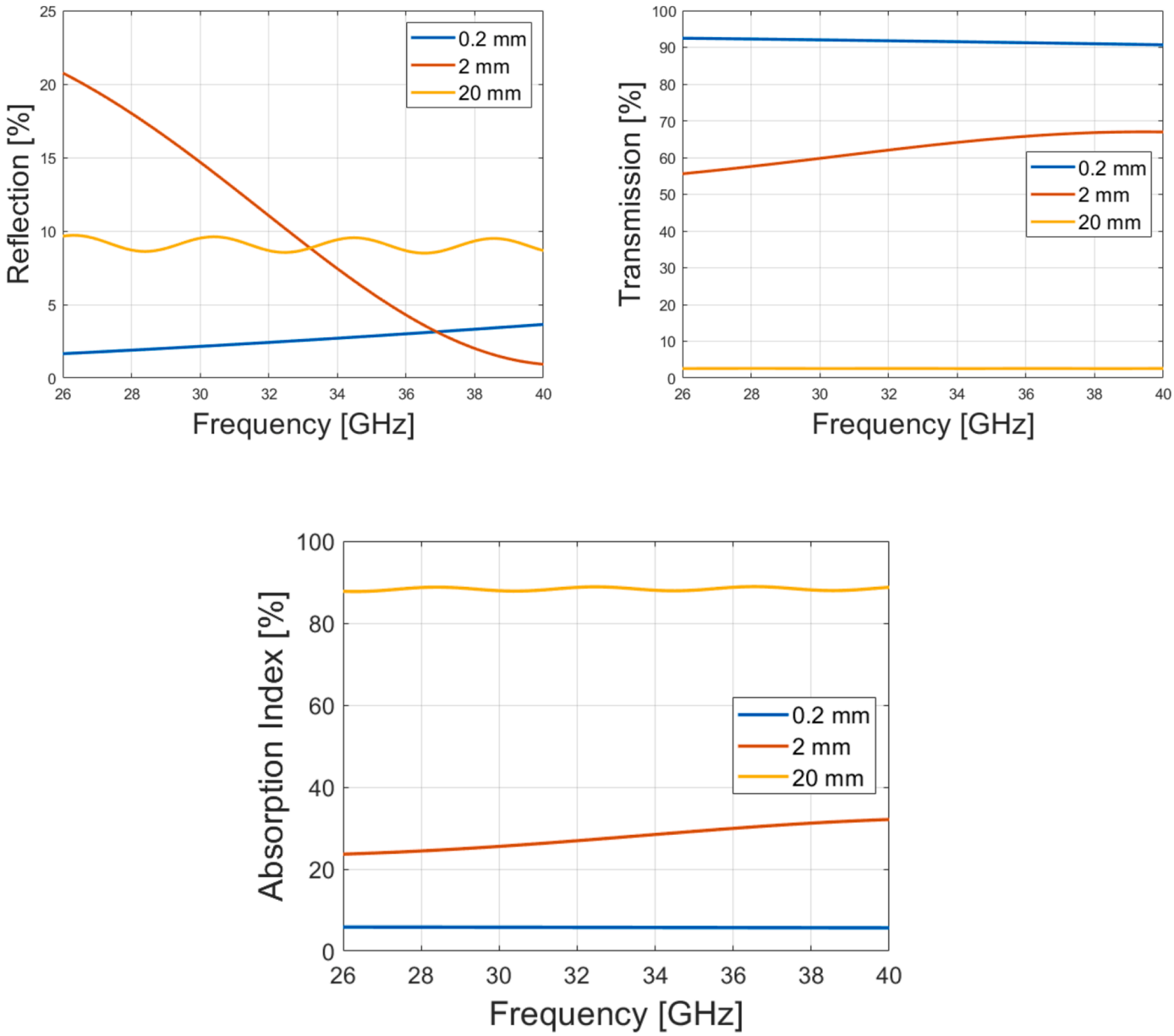

Fig. 8. Simulations based on the experimental data of rPLA-4OMMT of reflection, transmission and absorption index for a film thickness of 0.2, 2 and 20 mm.

the value of T at 26.5 GHz where a lowest value of 0.78 is reached, starting from 28 to 40 GHz, a similar trend can be seen on VPLA-2OMMT and VPLA. In case of rPLA, an increase of T is seen, since the value of T is as high as 0.85 in the whole studied frequency region. Which indicates that nanoclay contributes to the shielding mechanism when it is embedded in the recycled matrix. This behavior is more pronounced when higher amounts of nanoclays are introduced into VPLA as the value of T is higher than 0.90.

The absorption index gives the percentage of absorbed energy by the material. Fig. 7c shows a clear increase of absorption with higher nanoclay concentration. The nanoclays participate in the absorption because they raise the effective conductivity of the composite, hence allowing reaching up to 14.5 and 20.3% of average absorption on the measured VPLA-4OMMT and rPLA-4OMMT respectively. Mechanical recycling also significantly increases the absorption index. This phenomenon seems due to a shortening of the polymer chains during the reprocessing which results in a higher dielectric constant of the rPLA matrix (see Fig. 6), consequently an increase in reflection is observed in Fig. 7a while the transmission does not change.

Mechanical recycling of PLA combined with a high concentration of the nanoclay leads to relevant candidate for EMI shielding at microwave. Despite the good EM properties shown by the samples, the very thin film cannot reach high absorption levels since the wavelength is significantly higher than the thickness of the sample. Experimental data such as the complex permittivity of the nanocomposites allows simulating the EM behavior of the material having different thicknesses. Further explanations about the used method of chain matrix can be found in the literature [66]. Firstly, a film with 0.2mm-thick is simulated (see Fig. 8), matching the actual measurement of the rPLA-4OMMT sample. Then, a film of 2 mm was simulated, showing a transmission around 60%, which reaches relevant threshold for EMI shielding applications. An rPLA-4OMMT of 20 mm has an average absorption index of 90% and a quasi-zero transmission over the spectrum. Those simulations highlight the potential of the composites for shielding by absorption; this performance is also feasible thanks to the low reflection related to a good wave impedance matching.

4.5.3. Impedance matching

The propagating wave that comes at the input interface between air and a slab of composite material will undergo some reflection that is proportional to the magnitude of the difference between wave impedance of air and that of composite medium. The non-reflective materials have as primary function to absorb and dissipate the electromagnetic energy with high efficiency despite low thickness. The wave impedance of the PLA-OMMT nanocomposites varies in function of the frequency as shown as an example for the composite rPLA-4OMMT in Fig. 9. The wave impedance of air (displayed in dotted line on Fig. 9), $Z_0 = \sqrt{\frac{\mu_0}{\varepsilon_0}} \approx 377\ \Omega$, is constant. The wave impedance of the composite medium should be as close as possible to 377 Ω in order to avoid reflection; no homogeneous absorbing material is able to reach this value [67,68].

The average value over the spectrum of the wave impedance has been calculated and reported in Table 5 for all the composites. It can be observed that neither the presence of nanoclays nor the recycling process significantly affect the impedance, since the Z_w/Z_0 ratio stays near to 0.5. The virgin PLA-based composites show a slight increase, concretely the PLA-2OMMT film. Meanwhile the impedance ratio being roughly equal to 0.55 yields an input reflection coefficient expressing as $\Gamma = \frac{\frac{Z_w}{Z_0}-1}{\frac{Z_w}{Z_0}+1} \approx 0.3$. The fraction of power reflected at input interface being equal to $|\Gamma|^2$ has a value of roughly 10%. These values are in good agreement with those measured in Fig. 9.

The impedance matching concerns the interface between the air and the absorbing medium, the optimized solution is therefore a stack of the sample PLA-2OMMT followed by the best absorber i.e., rPLA-4OMMT as shown is Fig. 8. Such a structure appears as the best solution for EMI shielding from rPLA-based composites.

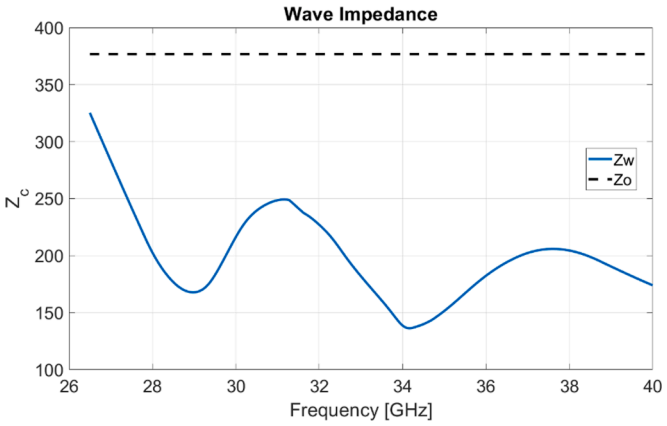

Fig. 9. Wave impedance of the rPLA-4OMMT composite. The dotted line is the theoretical impedance of vacuum.

Table 5
Average wave impedance at microwave frequency of the nanocomposites.

Sample	Z_w	Z_w/Z_0 ratio
PLA	200	0.53
PLA-2OMMT	212	0.57
PLA-4OMMT	192	0.51
rPLA	194	0.51
rPLA-2OMMT	183	0.49
rPLA-4OMMT	199	0.53

5. Conclusion

Virgin and recycled PLA and their composites reinforced by OMMT were obtained and analyzed with a focus on electromagnetic properties. The microstructure of the nanocomposites is only slightly affected by the recycling process. The FTIR, TGA and DSC characterization have shown that the mechanical recycling does not significantly affect the chemical properties of the PLA-composites. The presence of nanofillers also helps to maintain the performance of the non-recycled materials. The mechanical properties quantified by Vickers micro-hardness are consequently quite similar for each concentration of OMMT in VPLA or rPLA independently on the recycling process. The hardness goes from 184,79 up to 217 MPa depending on the OMMT concentration and an average increase of 5 MPa following the recycling process. Dielectric characterization has shown a significant gain in conductivity for the recycled PLA-based composites, while the dielectric constant stays steady for the set of measured samples. The rPLA-4OMMT film reaches 1.00 S/m and a dielectric constant of 3.5, while the equivalent composite VPLA-4OMMT gets 0.16 S/m and $\varepsilon_r'' = 3.3$. The EM properties are slightly affected by the aging and recycling processes. PLA-based composites 400 μm-thick exhibit higher microwave absorption of 14.5 and 20.3% for VPLA-4OMMT and rPLA-4OMMT, respectively. These nanocomposites can reach about 90% of absorption by simply increasing the thickness to 2 cm. The wave impedance of the panel of composites has been studied; the good impedance matching with the air makes them attractive EMI shielding materials. This set of results shows a serious advantage of using recycled PLA and their nanoclay biodegradable composites in terms of mechanical performances and EMI shielding efficiency. This work is a first step in the field of using recycled polymer nanocomposite.

Declaration of Competing Interest

The authors declare that they have no known competing financial interests or personal relationships that could have appeared to influence

the work reported in this paper.

Data availability

Data will be made available on request.

Acknowledgments

The authors are grateful to P. Simon and R. Jaiswar for their help in EM characterization and P. Bollen for fruitful discussions concerning experimental data extraction. As Research Director, prof. I. Huynen acknowledges the financial support of FNRS, Belgium. F.R. Beltrán and M.U. de la Orden acknowledge the support of the European Union's Horizon 2020 research and innovation program under grant agreement No. 860407 BIO-PLASTICS EUROPE, and the support of MINECO-Spain under project CTM2017–88989-P.

References

[1] J. Aniśko, M. Barczewski, P. Mietliński, A. Piasecki, J. Szulc, «Valorization of disposable polylactide (PLA) cups by rotational molding technology: the influence of pre-processing grinding and thermal treatment procedure,», Polym. Test. 107 (2022), 107481.
[2] N.F. Zaaba, M. Jaafar, «A review on degradation mechanisms of polylactic acid: hydrolytic, photodegradative, microbial, and enzymatic degradation,», Polymer Eng. Sci. 60 (19) (2020) 2061–2075, n°.
[3] W. Zou, J. Huang, J. Su, W. Zeng, Y. Liang, R. Chen, H. Zhang, Y. Min, Z. Gu, «Review on Modification of Poly (lactic acid) in Physical and Mechanical Properties,», ES Food Agrofor. 6 (2021) 3–11.
[4] E. Castro-Aguirre, F. Iniguez-Franco, H. Samsudin, X. Fang, R. Auras, «Poly (lactic acid)-Mass production, processing, industrial applications, and end of life,», Adv. Drug. Deliv. Rev. 107 (2016) 333–366.
[5] S.-.M. Huang, J.-.J. Hwang, H.-.J. Liu, A.-.M. Zheng, «A Characteristic Study of Polylactic Acid/Organic Modified Montmorillonite (PLA/OMMT) Nanocomposite Materials after Hydrolyzing,», cryst. 11 (14) (2021) 376, n°.
[6] L.A. Goettler, K.Y. Lee, H. Thakkar, «Layered silicate reinforced polymer nanocomposites: development and applications,», Polym. Rev. 47 (12) (2007) 291–317, n°.
[7] F. Uddin, Montmorillonite: An introduction to Properties and Utilization, IntechOpen, London, UK, 2018, pp. 3–23.
[8] K. Prakalathan, S. Mohanty, S.K. Nayak, «Polylactide/modified layered silicates nanocomposites: a critical analysis of morphological, mechanical and thermal properties,», J. Reinf. Plast. Compos. 31 (119) (2012) 1300–1310, n°.
[9] V.V. Krupskaya, S.V. Zakusin, E.A. Tyupina, O.V. Dorzhieva, M.S. Chernov, Y. V. Bychkova, «Transformation of structure and adsorption properties of montmorillonite under thermochemical treatment,», Geochem. Int. 57 (13) (2019) 314–330, n°.
[10] B. Mohd, A. Sahrim, R. Rozaidi, «Mechanical, thermal and morphological properties of poly(lactic acid)/natural rubber nanocomposites,», J. Reinf. Plast. Compos. 32 (121) (2013) 1656–1667, n°.
[11] T.T. Zhu, C.H. Zhou, F.B. Kabwe, Q.Q. Wu, C.S. Li, J.R. Zhang, «Exfoliation of montmorillonite and related properties of clay/polymer nanocomposites,», Appl. Clay Sci. 169 (2019) 48–66.
[12] R.U. Rao, B. Venkatanarayana, K.N.S. Suman, «Enhancement of mechanical properties of PLA/PCL (80/20) blend by reinforcing with MMT nanoclay,», Mater. Today: Proc. 18 (2019) 85–97.
[13] P. Ramesh, B.D. Prasad, K.L. Narayana, «Effect of MMT clay on mechanical, thermal and barrier properties of treated aloevera fiber/PLA-hybrid biocomposites,», Silicon 12 (17) (2020) 1751–1760, n°.
[14] S. Lee, M. Kim, H.Y. Song, K. Hyun, «Characterization of the effect of clay on morphological evaluations of PLA/biodegradable polymer blends by FT-rheology,», Macromolecules 52 (120) (2019) 7904–7919, n°.
[15] A. Mahmoodi, S. Ghodrati, M. Khorasani, «High-strength, low-permeable, and light-protective nanocomposite films based on a hybrid nanopigment and biodegradable PLA for food packaging applications,», ACS Omega 4 (112) (2019) 14947–14954, n°.
[16] J.L. Alves, P. d. T. V. e. Rosa, V. Realinho, M. Antunes, J.I. Velasco, A.R. Morales, «The effect of Brazilian organic-modified montmorillonites on the thermal stability and fire performance of organoclay-filled PLA nanocomposites,», Appl. Clay Sci. 194 (2020), 105697.
[17] M. Dadras Chomachayi, A. Jalali-Arani, F.R. Beltrán, M.U. de la Orden, J. Martínez Urreaga, «Biodegradable nanocomposites developed from PLA/PCL blends and silk fibroin nanoparticles: study on the microstructure, thermal behavior,developed from PLA/PCL blends and silk fibroin nanoparticles: study on the microstructure, thermal behavior, crystalli,», J. Polym. Environ. 28 (14) (2020) 1252–1264, n°.
[18] F.P. La Mantia, L. Botta, M. Morreale, R. Scaffaro, «Effect of small amounts of poly (lactic acid) on the recycling of poly (ethylene terephthalate) bottles,», Polym. Degrad. Stab. 97 (11) (2012) 21–24, n°.
[19] S.M. Al-Salem, P. Lettieri, J. Baeyens, «Recycling and recovery routes of plastic solid waste (PSW): a review,», Waste Manage. (Oxford) 29 (110) (2009) 2625–2643, n°%.
[20] J.D. Badia, O. Gil-Castell, A. Ribes-Greus, «Long-term properties and end-of-life of polymers from renewable resources,», Polym. Degrad. Stab. 137 (2017) 35–57.
[21] J.D. Badia, A. Ribes-Greus, «Mechanical recycling of polylactide, upgrading trends and combination of valorization techniques,», Eur. Polym. J. 84 (2016) 22–39.
[22] H. Kometani, T. Matsumura, T. Suga, T. Kanai, «Quantitative analysis for polymer degradation in the extrusion process,», Int. Polym. Proc. 21 (11) (2009) 24–31, n°.
[23] F. Vilaplana, S. Karlsson, «Quality concepts for the improved use of recycled polymeric materials: a review,», Macromol. Mater. Eng. 293 (14) (2008) 274–297, n°.
[24] R. Jaiswar, Y. Danlée, H. Mesfin, A. Delcorte, S. Hermans, C. Bailly, J.-.P. Raskin, I. Huynen, «Absorption modulation of FSS-polymer nanocomposites through incorporation of conductive nanofillers,», Appl. Phys. A 123 (1164) (2017) n°.
[25] G. Kister, G. Cassanas, M. Vert, «Effects of morphology, conformation and configuration on the IR and Raman spectra of various poly(lactic acid)s,», Polymer (Guildf) 39 (12) (1998) 267–273, n°.
[26] I.S. Ristić, L. Tanasić, L.B. Nikolić, S.M. Cakić, O.Z. Ilić, R.Ž. R.adičević, J. K. Budinski-Simendić, «The properties of poly (L-lactide) prepared by different synthesis procedure,», J. Polym. Environ. 19 (12) (2011) 419–430, n°.
[27] F.R. Beltrán, V. Lorenzo, M.U. De la Orden, J. Martínez-Urreaga, «Effect of different mechanical recycling processes on the hydrolytic degradation of poly (l-lactic acid),», Polym. Degrad. Stab. 133 (2016) 339–348.
[28] T.G. Mayerhöfer, J. Popp, «The electric field standing wave effect in infrared transflection spectroscopy,», Spectrochim. Acta Part A 191 (2018) 283–289.
[29] M.K.M. Haafiz, A. Hassan, Z. Zakaria, I.M. Inuwa, M.S. Islam, M. Jawaid, «Properties of polylactic acid composites reinforced with oil palm biomass microcrystalline cellulose,», Carbohydr. Polym. 98 (2013) 139–145.
[30] J.D. Badia, E. Strömberg, S. Karlsson, A. Ribes-Greus, «Material valorisation of amorphous polylactide. Influence of thermo-mechanical degradation on the morphology, segmental dynamics, thermal and mechanical performance,», Polym. Degrad. Stab. 97 (14) (2012) 670–678, n°.
[31] F.R. Beltrán, E. Ortega, A.M. Solvoll, V. Lorenzo, M.U. de la Orden, J. Martínez Urreaga, «Effects of aging and different mechanical recycling processes on the structure and properties of poly (lactic acid)-clay nanocomposites,», J. Polym. Environ. 26 (15) (2018) 2142–2152, n°.
[32] X. Huang, W. Brittain, «Synthesis and Characterization of PMMA nanocomposite by suspension and emulsion polymerization,», Macromolecules 34 (110) (2001) 3255–3260, n°.
[33] F.R. Beltrán, V. Lorenzo, J. Acosta, M.U. de la Orden, J.M. Urreaga, «Effect of simulated mechanical recycling processes on the structure and properties of poly (lactic acid),», J. Environ. Manage. 216 (2018) 25–31.
[34] W. Chow, S. Lok, «Thermal properties of poly (lactic acid)/organo-montmorillonite nanocomposites,», J. Therm. Anal. Calorim. 95 (12) (2009) 627–632, n°.
[35] J.L. Feijoo, L. Cabedo, E. Gimenez, J.M. Lagaron, J.J. Saura, «Development of amorphous PLA-montmorillonite nanocomposites,», J. Mater. Sci. 40 (17) (2005) 1785–1788, n°.
[36] T.M. Wu, C.Y. Wu, «Biodegradable poly (lactic acid)/chitosan-modified montmorillonite nanocomposites: preparation and characterization,», Polym. Degrad. Stab. 91 (19) (2006) 2198–2204, n°.
[37] K. Fukushima, D. Tabuani, M. Dottori, I. Armentano, J.M. Kenny, G. Camino, «Effect of temperature and nanoparticle type on hydrolytic degradation of poly (lactic acid) nanocomposites,», Polym. Degrad. Stab. 96 (112) (2011) 2120–2129, n°.
[38] S.M. Lai, S.H. Wu, G.G. Lin, T.M. Don, «Unusual mechanical properties of melt-blended poly (lactic acid)(PLA)/clay nanocomposites,», Eur. Polym. J. 52 (2014) 193–206.
[39] A.B. Gomez-Gamez, A. Yebra-Rodriguez, A. Peñas-Sanjuan, B. Soriano-Cuadrado, J. Jimenez-Millan, «Influence of clay percentage on the technical properties of montmorillonite/polylactic acid nanocomposites,», Appl. Clay Sci. 198 (2020), 105818.
[40] M.L. Di Lorenzo, «Calorimetric analysis of the multiple melting behavior of poly (L-lactic acid),», J. Appl. Polym. Sci. 100 (14) (2006) 3145–3151, n°.
[41] C. Thellen, C. Orroth, D. Froio, D. Ziegler, J. Lucciarini, R. Farrell, N.A. D'Souza, J. A. Ratto, «Influence of montmorillonite layered silicate on plasticized poly (l-lactide) blown films,», Polymer (Guildf) 46 (125) (2005) 11716–11727, n°.
[42] S. Molinaro, M.C. Romero, M. Boaro, A. Sensidoni, C. Lagazio, M. Morris, J. Kerry, «Effect of nanoclay-type and PLA optical purity on the characteristics of PLA-based nanocomposite films,», J. Food Eng. 117 (11) (2013) 113–123, n°.
[43] M. Yourdkhani, T. Mousavand, N. Chapleau, P. Hubert, «Thermal, oxygen barrier and mechanical properties of polylactide–organoclay nanocomposites,», Compos. Sci. Technol. 82 (2013) 47–53.
[44] F. Li, C. Zhang, Y. Weng, «Improvement of the Gas Barrier Properties of PLA/OMMT Films by Regulating the Interlayer Spacing of OMMT and the Crystallinity of PLA,», ACS Omega 5 (130) (2020) n°.
[45] P. Krishnaiah, C.T. Ratnam, S. Manickam, «Development of silane grafted halloysite nanotube reinforced polylactide nanocomposites for the enhancement of mechanical, thermal and dynamic-mechanical properties,», Appl. Clay Sci. 135 (2017) 583–595.
[46] F.R. Beltrán, M.U. De La Orden, J. Martínez Urreaga, «Amino-modified halloysite nanotubes to reduce polymer degradation and improve the performance of mechanically recycled poly (lactic acid),», J. Polym. Environ. 26 (110) (2018) n°.
[47] O.M. Sanusi, A. Benelfellah, L. Papadopoulos, Z. Terzopoulou, L. Malletzidou, I. G. Vasileiadis, K. Chrissafis, D.N. Bikiaris, N.A. Hocine, «Influence of

montmorillonite/carbon nanotube hybrid nanofillers on the properties of poly (lactic acid),», Appl. Clay Sci. 201 (2021), 105925.
[48] F.J. Calleja, D.S. Sanditov, V.P. Privalko, «The microhardness of non-crystalline materials,», J. Mater. Sci. 37 (121) (2002) 4507–4516, n°.
[49] H. Wu, F. Dave, M. Mokhtari, M.M. Ali, R. Sherlock, A. McIlhagger, D. Tormey, S. McFadden, «On the Application of Vickers Micro Hardness Testing to Isotactic Polypropylene,», Polymers (Basel) 14 (19) (2022) n°.
[50] J. Aurrekoetxea, M.A. Sarrionandia, I. Urrutibeascoa, M.L. Maspoch, «Effects of injection moulding induced morphology on the fracture behaviour of virgin and recycled polypropylene,», Polymer (Guildf) 44 (122) (2003) 6959–6964, n°.
[51] H.A. Lutpi, H. Anuar, N. Samat, S.N. Surip, N.N. Bonnia, «Evaluation of elastic modulus and hardness of polylactic acid-based biocomposite by nano-indentation,», Adv. Mat. Res. 576 (2012) 446–449.
[52] M.S. Saharudin, R. Atif, I. Shyha, F. Inam, «The degradation of mechanical properties in halloysite nanoclay–polyester nanocomposites exposed to diluted methanol,», J. Compos. Mater. 51 (111) (2017) 1653–1664, n°.
[53] Y. Danlée, C. Bailly, I. Huynen, L. Piraux, «Flexible multilayer combining nickel nanowires and polymer films for broadband microwave absorption,», IEEE Trans. Electromagn. Compat. 62 (15) (2019) 1661–1668, n°.
[54] R. McKenzie, W. Zurawsky, J. Mijovic, «A molecular interpretation of Maxwell–Wagner–Sillars processes,», J. Non Cryst. Solids 406 (2014) 11–21. *406, 11-21*.
[55] J.K. Jeszka, L. Pietrzak, M. Pluta, G. Boiteux, «Dielectric properties of polylactides and their nanocomposites with montmorillonite,», J. Non Cryst. Solids 356 (111–17) (2010) 818–821, n°.
[56] D. Yu, J. Wu, L. Zhou, D. Xie, S. Wu, «The dielectric and mechanical properties of a potassium-titanate-whisker-reinforced PP/PA blend,», Compos. Sci. Technol. 60 (14) (2000) 499–508, n°.
[57] A. Saib, L. Bednarz, R. Daussin, C. Bailly, X. Lou, J.-.M. Thomassin, C. Pagnoulle, C. Detrembleur, R. Jérôme, I. Huynen, «Carbon Nanotube Composites for Broadband Microwave Absorbing Materials,», IEEE Trans. Microw. Theory Tech. 54 (16) (2006) 2745–2754, n°.
[58] L. Ben Ammar, H. Hammami, S. Fakhfakh, S. Taktak, «Impact of nanoclay loading on the structural, thermal and dielectric properties of montmorillonite/polypropylene nanocomposites,», Polym. Compos. 42 (15) (2021) 2492–2501, n°.
[59] L. Yu, P. Cebe, «Effect of nanoclay on relaxation of poly (vinylidene fluoride) nanocomposites,», J. Polym. Sci. Part B Polym. Phys. 47 (124) (2009) 2520–2532, n°.
[60] N.J.S. Sohi, M. Rahaman, D. Khastgir, «Dielectric property and electromagnetic interference shielding effectiveness of ethylene vinyl acetate-based conductive composites: effect of different type of carbon fillers,», Polym. Compos. 32 (17) (2011) 1148–1154, n°.
[61] V. Kumar, N.K. Sharma, R. Kumar, «Dielectric, mechanical, and thermal properties of bamboo–polylactic acid bionanocomposites,», J. Reinf. Plast. Compos. 31 (11) (2013) 42–51, n°.
[62] J.-.Y. Kim, W.H. Lee, J.W. Suk, J.R. Potts, H. Chou, I.N. Kholmanov, R.D. Piner, J. Lee, D. Akinwande, R.S. Ruoff, «Chlorination of reduced graphene oxide enhances the dielectric constant of reduced graphene oxide/polymer composites,», Adv. Mater. 25 (116) (2013) 2308, n°.
[63] L. Sidi Salah, M. Chouai, Y. Danlée, I. Huynen, N. Ouslimani, «Simulation and Optimization of Electromagnetic Absorption of Polycarbonate/CNT Composites Using Machine Learning.,», Micromachines (Basel) 11 (18) (2020) 778, n°.
[64] M.M. Jalili, S. Moradian, «Deterministic performance parameters for an automotive polyurethane clearcoat loaded with hydrophilic or hydrophobic nano-silica,», Prog. Org. Coat. 66 (14) (2009) 359–366, n°.
[65] A. Harish Kumar, M.B. Ahamed, K. Deshmukh, M.S. Sirajuddeen, «Morphology, dielectric and EMI shielding characteristics of graphene nanoplatelets, montmorillonite nanoclay and titanium dioxide nanoparticles reinforced polyvinylidenefluoride nanocomposites,», J. Inorg. Organomet. Polym. Mater. 31 (15) (2021) 2003–2016, n°.
[66] J.-.M. Thomassin, C. Jérôme, T. Pardoen, C. Bailly, I. Huynen, C. Detrembleur, «Polymer/carbon based composites as electromagnetic interference (EMI) shielding materials,», Mater. Sci. Eng. R Rep. 74 (17) (2013) 211–232, n°.
[67] P.S. Neelakanta, Handbook of Electromagnetic materials: Monolithic and Composite Versions and Their Applications, CRC press, 1995.
[68] X. Tong, Advanced Materials and Design For Electromagnetic Interference Shielding, CRC press, 2016.